Modern Physics Letters B, Vol. 23, No. 27 (2009) 3191–3207

World Scientific
www.worldscientific.com

MIXED-ORDER KINETICS MODEL FOR OPTICALLY STIMULATED LUMINESCENCE

G. KITIS*
Aristotle University of Thessaloniki, Nuclear Physics Laboratory, 541 24 Thessaloniki, Greece
gkitis@auth.gr

C. FURETTA
Touro University Rome, Circne Gianicolense 15-17, 00153 Rome, Italy
c.furetta@alice.it

V. PAGONIS
Physics Department, McDaniel College, Westminster, MD 21157, USA
vpagonis@mcdaniel.edu

Received 5 May 2008
Revised 7 July 2008

The theory of mixed-order kinetics is well-established for the description of single thermoluminescence (TL) glow-peaks. The main advantage of mixed-order kinetics relative to the more widely used general-order kinetic theory is that the former is physically meaningful whereas the latter is entirely empirical. In the case of optically stimulated luminescence (OSL) either non-first-order or second-order kinetics are studied using the empirical general-order kinetics theory. In the present work, expressions for mixed-order kinetics are derived for OSL curves. A peak shape parameter for linear modulation OSL is developed and special mixed-order expressions are derived for use in the computerized OSL curve deconvolution analysis.

Keywords: OSL; LM-OSL; CW-OSL.

1. Introduction

Optically stimulated luminescence (OSL) signals are usually measured using two different techniques, namely continuous wave OSL (CW-OSL)and linearly modulated OSL (LM-OSL). In the former case, one keeps the light stimulation intensity constant, and the OSL signal usually decays with time. In the latter case the stimulation intensity is linearly ramped from zero up to a specific maximum intensity, and the measured LM-OSL signal is a peak-shaped curve, analogous to a TL glow-peak measured with a linear heating function. Bulur,[1] suggested the LM-OSL technique of measuring OSL and gave the mathematical formulation of LM-OSL curves

*Corresponding author.

for first, second and general-order kinetics. Later, Bulur[2] proposed a method to transform a CW-OSL curve into a LM-OSL curve called a Pseudo-LM-OSL curve (PS-LM-OSL).

To the best of our knowledge, the physically meaningful mixed-order kinetics has never been studied in the case of OSL processes. The aims of the present work are:

(i) to find mixed-order expressions for a single OSL curve for both CW-OSL and LM-OSL,
(ii) to find an expression for the PS-LM-OSL transformation of a CW-OSL curve,
(iii) to investigate the LM-OSL peak shape parameters, and
(iv) to derive mixed-order kinetics LM-OSL expressions to use in the Computerized Curve Deconvolution Analysis (CCDA).

Finally, our goal is to compare the results of using the developed mixed-order expressions with the widely used, but empirically based, general-order expressions.

2. Theory

The simplest phenomenological model describing a single TL glow-peak consists of one main active trap (AT) and one recombination center (RC). This is known as the one trap and one recombination center model (OTOR).[3] Other models take into account additional electron traps and recombination centers which usually exist in most materials. Representatives examples of such models are the interactive multi-trap system (IMTS) and non-interactive multi trap system (NMTS) models,[4] which in addition to the main AT contain also a thermally disconnected deep trap (TDDT). The TDDT is assumed to remains unaffected by heating of the sample which causes the active trap to empty. The energy band diagram describing such models is shown in Fig. 1.

According to the band energy model of Fig. 1, the traffic of electrons during the LM-OSL stimulation stage is described by the following set of differential rate

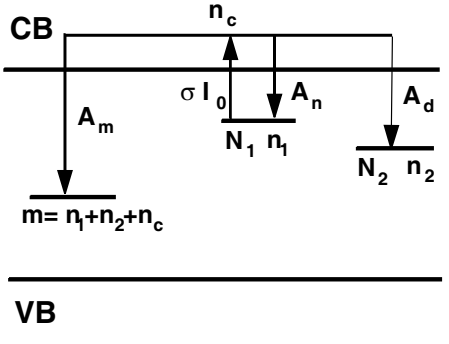

Fig. 1. Energy band model diagram.

equations:

$$\frac{dn_1}{dt} = -n_1 gt + n_c(N_1 - n_1)A_n\,, \tag{1}$$

$$\frac{dn_2}{dt} = n_c(N_2 - n_2)A_d\,, \tag{2}$$

$$\frac{dn_c}{dt} = n_1 gt - n_c(N_1 - n_1)A_n - n_c(N_2 - n_2)A_d - n_c(n_1 + n_2 + n_c)A_m\,. \tag{3}$$

The OSL intensity is given by

$$I = -\frac{dn_1}{dt} - \frac{dn_2}{dt} - \frac{dn_c}{dt} = n_c(n_1 + n_2 + n_c)A_m\,, \tag{4}$$

where N_1 and n_1 are the concentrations of the total and of the filled active trap (AT), N_2 and n_2 are the concentrations of the TDDT, and n_c the concentration of electrons in the conduction band. The concentration m of the recombination centers (RC) is equal to $m = n_1 + n_2 + n_c$, so that the charge balance of the system is maintained. A_n, A_d, and A_m are the capture coefficients for the AT, TDDT and RC respectively. The parameter g is equal to $\sigma I_0/T$, with σ representing the cross-section for optical stimulation, I_0 the stimulation intensity and T the total OSL simulation time. The OSL decay constant λ is defined as $\lambda = \sigma I_0$.

The above system of rate equations describes the IMTS model.[4] When the condition $n_{20} = N_2$ is satisfied, the TDDT is saturated and cannot capture free carriers. This is known as the NMTS limit of the IMTS model. When the condition $n_{10} \gg n_{20} = N_2$ is satisfied, this is known as the OTOR limit of the NMTS model. The condition $n_{20} = N_2 = A_d = 0$ defines the pure OTOR model. Here n_{10} and n_{20} are the concentration of the AT and the TDDT correspondingly at time $t = 0$.

Unfortunately, the above rate equations cannot be solved analytically. However, by making certain simplifying physical assumptions, it is possible to arrive at analytical expressions for the LM-OSL intensity. The first assumption is the quasi-equilibrium condition (QEC), according to which the concentration of electrons in the conduction band is always negligible relative to their concentrations in electron traps.[3] The QEC is expressed by the relation

$$\left|\frac{dn_c}{dt}\right| \ll \left|\frac{dn_1}{dt}\right|, \left|\frac{dn_2}{dt}\right|, \left|\frac{dm}{dt}\right|. \tag{5}$$

By applying the QEC to the OTOR model, the "general one trap one recombination center" equation for the LM-OSL intensity can be derived. From this model, the known first[1] and second kinetics order[1] analytical expressions can be obtained under some restrictive assumptions.

In the case of the NMTS model, the TDDT is assumed to be initially saturated, i.e. $n_{20} = N_2$. By further assuming that $dn_2/dt \simeq 0$, Eq. (3) can be solved with

respect to n_c, which can be replaced in Eq. (4). In this manner, the following general "two trap one recombination center" equation is obtained:

$$I_{OSL} = n_1 \cdot g \cdot t \cdot \frac{(n_1 + n_2)A_m}{(N_1 - n_1)A_n + (n_1 + N_2)A_m} \,. \tag{6}$$

For slow re-trapping $(N_1 - n_1)A_n \ll (n_1 + N_2)A_m$ and Eq. (6) leads directly to the expression for first-order kinetics.

Alternatively, in the case of fast re-trapping the condition $(N_1 - n_1)A_n \gg (n_1 + N_2)A_m$, along with $n_1 \ll N_1$, leads to the following expression for the OSL intensity:

$$I_{OSL} = n_1 \cdot g \cdot t \cdot \frac{(n_1 + N_2)A_m}{N_1 A_n} \,. \tag{7}$$

For the special case of $A_n = A_m$, we see that Eq. (6) becomes

$$I_{OSL} = n_1 \cdot g \cdot t \cdot \frac{n_1 + N_2}{N_1 + N_2} \,. \tag{8}$$

Both Eqs. (7) and (8) can be presented in the form

$$I_{OSL} = g' \cdot n_1(n_1 + N_2) \cdot t \,, \tag{9}$$

with $g' = g/N_1$ or $g' = g/(N_1 + N_2)$ respectively. The last equation is the general form of the OSL intensity for mixed order kinetics.

2.1. *Mixed-order LM-OSL equation*

The mixed-order equation for LM-OSL can be derived by considering that $I_{OSL} = -dm/dt \approx -dn_1/dt$ and by solving the following differential equation:

$$-\frac{dn_1}{dt} = g' \cdot n_1(n_1 + N_2) \cdot t \,. \tag{10}$$

After integration and a little algebra, the following expression is obtained:

$$ln\left(\frac{n_1 + N_2}{n_1} \cdot \frac{n_{10}}{n_{10} + N_2}\right) = N_2 \cdot g' \cdot \frac{t^2}{2} \,. \tag{11}$$

At this point, we insert the mixed-order parameter α defined as

$$\alpha = \frac{n_{10}}{n_{10} + N_2} \,. \tag{12}$$

Hence, from Eq. (11) it is found that

$$n_1 = \frac{\alpha \cdot N_2}{F(t) - \alpha} \,, \tag{13}$$

with

$$F(t) = \exp\left(N_2 \cdot g' \cdot \frac{t^2}{2}\right) . \tag{14}$$

By inserting n_1 from Eq. (13) in Eq. (10), the following mixed-order expression for LM-OSL is obtained:

$$I(t) = g' \cdot t \cdot \frac{\alpha \cdot N_2^2 \cdot F(t)}{(F(t) - \alpha)^2} \,. \tag{15}$$

For the needs of numerical simulation, the terms $g'n_2$ and $g'\alpha n_2^2$ must be further analyzed. By substituting the value of n_2 from Eq. (12) we have

$$g' \cdot \alpha \cdot N_2^2 = \frac{\lambda}{T} \cdot \frac{1}{N_1 + N_2} = \frac{\lambda}{T} \cdot n_{10} \cdot (1 - \alpha)^2 \cdot G\left(\frac{n_{10}}{N_1}\right), \tag{16}$$

with

$$G\left(\frac{n_{10}}{N_1}\right) = \frac{n_{10}/N_1}{\alpha + (1 - \alpha)(n_{10}/N1)} \,. \tag{17}$$

For $n_{10} = N_1$, the value of $G(n_{10}/N_1) = 1$.

Working in a similar manner it is found that

$$g' \cdot N_2 = \frac{\lambda}{T} \cdot (1 - \alpha) \cdot G\left(\frac{n_{10}}{N_1}\right). \tag{18}$$

From the general expression of the LM-OSL mixed-order kinetics given by Eq. (15), the condition for the maximum can be obtained by equating its derivative to zero. The condition for the maximum of LM-OSL peak is found to be:

$$t_m^2 = \frac{T}{\lambda} \cdot \frac{1}{1 - \alpha} \cdot \frac{F_m - \alpha}{F_m + \alpha} \,, \tag{19}$$

where F_m is the value of F(t) given by Eq. (14) at $t = t_m$.

This condition for the maximum is an implicit function of t_m, since the expression for F_m in Eq. (14) contains t_m. A similar implicit relationship was found previously in the case of a mixed-order model for Thermoluminescence.[7]

2.2. *Mixed-order CW-OSL equation*

In the case of CW-OSL, Eq. (10) will take the form

$$\frac{dn_1}{dt} = \lambda' \cdot n_1(n_1 + N_2) \,. \tag{20}$$

The solution of Eq. (20) is

$$I(t) = \lambda' \cdot t \cdot \frac{\alpha \cdot N_2^2 \cdot F(t)}{(F(t) - \alpha)^2} \,, \tag{21}$$

which, is exactly similar with Eq. (15), but with the function $F(t)$ given by Eq. (14) taking now the following form:

$$F(t) = \exp(\lambda' \cdot N_2 \cdot t) \,. \tag{22}$$

Here $\lambda' = \lambda/N_1$ or $\lambda' = \lambda/(N_1 + N_2)$ respectively (as in Eqs. (7)–(9)). These terms can be analyzed in the same manner as Eqs. (16) and (18).

2.3. *Transformation of a CW-OSL decay curve into a pseudo LM-OSL peak-shaped curve*

The transformation of a CW-OSL curve into a peak shaped curve called PS-LM-OSL, is easily done by following the derivation of Bulur.[2] A new independent variable u is introduced, i.e.

$$u = \sqrt{2tP} \quad \text{or} \quad t = \frac{u^2}{2T}\,, \tag{23}$$

with u having the units of time and T representing the total stimulation time.

By substituting Eq. (23) into Eq. (21) and further multiplying Eq. (21) by u/T, the following PS-LM-OSL equation is obtained, i.e.

$$I(u) = \lambda' \cdot u \cdot \frac{\alpha \cdot N_2^2 \cdot F(u)}{(F(u) - \alpha)^2}\,, \tag{24}$$

with

$$F(u) = \exp\left(\lambda' \cdot N_2 \cdot \frac{u^2}{2}\right). \tag{25}$$

2.4. *Properties of the peak parameters for LM-OSL peaks*

A single TL or LM-OSL peak can be characterized using the peak shape parameters. These are based on certain geometrical characteristics, namely the peak maximum time t_m, and the times at half-maximum LM-OSL intensity t_1 and t_2 on the two sides of the LM-OSL peak. These quantities are used to define further the widths $\omega = t_1 - t_2$, $\delta = t_2 - t_m$ and $\tau = t_m - t_1$, as well as the symmetry factor of the glow-peak $\mu_g = \delta/\omega$, which is commonly referred to as the geometrical symmetry factor.

The derivation of the existing peak shape parameters is based on the so-called triangle assumption, which can be expressed in three different ways, each one leading to an individual family of peak shape parameters. In the form given by Chen,[5] these are

$$C_\omega = \frac{\omega I_m}{n_{10}} \tag{26}$$

$$C_\delta = \frac{\delta I_m}{n_{1m}} \tag{27}$$

$$C_\tau = \frac{\tau I_m}{n_{10} - n_{1m}} \tag{28}$$

with

$$n_{1m} = \int_{t_m}^{\infty} I dt\,, \tag{29}$$

where I_m is the peak maximum intensity, n_{1m} represents the high-time half-integral of the LM-OSL peak and C_ω, C_δ and C_τ are quantities which characterize the degree

by which the area of a single LM-OSL peak approaches the area of a triangle. These quantities were found to vary extremely slowly in the case of TL and they are known as pseudo-constants in that case.

In order to derive the peak parameters formulas using Eqs. (26)–(28), one has to evaluate the terms I_m/n_{10}, n_{1m}/n_{10} and I_m/n_{1m} from the analytical LM-OSL expressions.

By using Eqs. (16) and (18) for $t = t_m$, Eq. (15) becomes

$$I_m = n_{10} \cdot \frac{\lambda}{T} \cdot t_m \cdot (1-\alpha)^2 \cdot \frac{F_m}{(F_m-\alpha)^2} \,. \tag{30}$$

Furthermore, by taking into account the condition for the maximum given by Eq. (19), the term I_m/n_{10} is given by the following expression:

$$\frac{I_m}{n_{10}} = \frac{1-\alpha}{t_m} \cdot \frac{F_m}{F_m^2-\alpha^2} \,. \tag{31}$$

Using the definition of Eq. (29), Eq. (13) can be written as

$$n_{1m} \cdot (F_m - \alpha) = \alpha \cdot N_2 \,. \tag{32}$$

By substituting n_{20} from Eq. (12) into Eq. (32), we obtain the term n_{1m}/n_{10},

$$\frac{n_{1m}}{n_{10}} = \frac{1-\alpha}{F_m-\alpha} = \mu_g' \,. \tag{33}$$

The last quantity in Eq. (33) is known as the integral symmetry factor μ_g', and has exactly the same form as in the case of TL.[6]

By dividing Eq. (31) and Eq. (33), one obtains the term I_m/n_{1m},

$$\frac{I_m}{n_{1m}} = \frac{1}{t_m} \cdot \frac{F_m}{F_m+\alpha} \,. \tag{34}$$

Once the terms I_m/n_{10}, n_{1m}/n_{10} and I_m/n_{1m} have been evaluated, one can proceed to the evaluation of the LM-OSL peak parameters.

By substituting Eq. (31) in Eq. (26) and after some algebra, the following relation between t_m and ω is obtained:

$$\frac{\omega}{t_m} = C_\omega \cdot \frac{1}{\mu_g'} \cdot \frac{F_m+\alpha}{F_m} \,. \tag{35}$$

Similarly, by substituting Eq. (33) into Eq. (27), the following relation between δ and t_m is obtained:

$$\frac{\delta}{t_m} = C_\delta \cdot \frac{F_m+\alpha}{F_m} \,. \tag{36}$$

Equation (28) can be written as

$$\frac{n_{10}}{n_{1m}} - 1 = \frac{\tau}{C_\tau} \cdot \frac{I_m}{n_{1m}} \,. \tag{37}$$

Table 1. Symmetry factors (geometrical and integral) and kinetic parameters of mixed-order LM-OSL peaks.

α	μ_g	μ'_g	F_m	b
0.01	0.576	0.608	1.6397	1.005
0.05	0.581	0.613	1.6005	1.028
0.1	0.586	0.620	1.5527	1.060
0.2	0.600	0.634	1.4621	1.130
0.3	0.614	0.649	1.3792	1.209
0.4	0.626	0.664	1.3039	1.296
0.5	0.638	0.679	1.2364	1.393
0.6	0.648	0.694	1.1763	1.498
0.7	0.656	0.709	1.1232	1.612
0.8	0.662	0.723	1.0765	1.735
0.9	0.665	0.737	1.0357	1.864
0.94	0.666	0.742	1.0208	1.918
0.98	0.666	0.747	1.0068	1.971

Finally, by substituting Eqs. (33) and (34) in Eq. (37), the following relation between τ and t_m is obtained:

$$\frac{\tau}{t_m} = C_\tau \cdot \frac{1-\mu'_g}{\mu'_g} \cdot \frac{F_m+\alpha}{F_m} \,. \tag{38}$$

By taking into account Eq. (33), the term F_m is evaluated as

$$F_m = \frac{1+\alpha(\mu'_g-1)}{\mu'_g} \,. \tag{39}$$

By using Eq. (39), the common term appearing in Eqs. (35), (36) and (38) can be written as

$$\frac{F_m+\alpha}{F_m} = \frac{1+\alpha(2\mu'_g-1)}{1+\alpha(\mu'_g-1)} \,. \tag{40}$$

3. Deconvolution Equation for LM-OSL

Experimental LM-OSL curves usually consist of several overlapping peaks. The separation of a complex LM-OSL curve into its individual components is achieved by a computerized curve deconvolution analysis (CCDA). The single LM-OSL peak expressions for the CCDA are those given by Eq. (15). The free parameters for the CCDA are n_{10}, α and λ. The CCDA fitting procedure starts by assuming some initial guess values for the free parameters n_{10}, α and λ, which cannot be extracted directly from the experimental LM-OSL curve. It is possible to transform the $I(n_{10}, \alpha, \lambda, t)$ expressions into new expressions depending upon variables which

can be extracted directly from the experimental LM-OSL curve, specifically into the form $I(I_m, t_m, \alpha, t)$ which depends on the quantities I_m and t_m.

By substituting the term $\lambda(1-\alpha)/T$ from the condition for the maximum given by Eq. (19) into Eq. (15), the following expression is obtained:

$$I(t) = n_{10} \cdot (1-\alpha) \cdot \frac{t}{t_m^2} \cdot \frac{F_m - \alpha}{F_m + \alpha} \cdot \frac{F(t)}{(F(t)-\alpha)^2} \,. \tag{41}$$

By substituting the term $n_{10}(1-\alpha)/t_m$ from Eq. (31) into Eq. (41), we obtain the expression

$$I(t) = I_m \cdot \frac{t}{t_m} \cdot \left(\frac{F_m - \alpha}{F(t) - \alpha} \right)^2 \cdot \frac{F(t)}{F_m} \,, \tag{42}$$

with

$$F(t) = \exp\left(\frac{1}{2} \cdot \frac{t^2}{t_m^2} \cdot \frac{F_m - \alpha}{F_m + \alpha} \right), \tag{43}$$

and

$$F_m = \exp\left(\frac{1}{2} \cdot \frac{F_m - \alpha}{F_m + \alpha} \right). \tag{44}$$

Equation (42) cannot be used easily in its present form, but it can be brought into a more useful form in two different ways. In the first technique, a relation between F_m and α is found by a numerical simulation, as described in a subsequent section. Based on this relation between F_m and α, the term F_m can be replaced by α in Eqs. (43) and (44), so that Eq. (42) will be transformed into a three-parameter function, i.e. $I(I_m, t_m, \alpha, t)$.

Alternatively, one can use the term F_m from Eq. (39) and replace it in Eqs. (43) and (44), obtaining the following expressions:

$$F(t) = \exp\left(\frac{1}{2} \cdot \frac{t^2}{t_m^2} \cdot \frac{1-\alpha}{1 + \alpha(\mu_g' - 1)} \right), \tag{45}$$

$$F_m = \left(\frac{1}{2} \cdot \frac{1-\alpha}{1 + \alpha(\mu_g' - 1)} \right). \tag{46}$$

Therefore, using Eqs. (45) and (46), Eq. (42) is transformed into a four-parameter equation, i.e. $I\ (I_m, t_m, \mu_g', \alpha, t)$. It must be noticed that in both cases the implicit function F_m is removed.

The computerized deconvolution of complex spectra is widely used for TL glow-curves. However, two major problems exist. The first problem is the existence of very closely spaced glow-peaks, which is a common problem for the analysis of any type of spectrum. The second problem is that every peak maximum temperature T_m corresponds, theoretically, to an infinite number of pairs of activation energy E and frequency factor s. The main consequence of these two problems is that it is difficult in the case of TL to obtain a unique solution.

The situation is different in the case of LM-OSL curves. The reason is that as it is seen from Eq. (19), for the given measuring conditions, the time maximum t_m depends only on one parameter (λ) and not on two parameters (E and s), as in the case of TL. Therefore, for a given total stimulation time T, the respective value of t_m corresponds to one and only one peak. In the case of mixed-order kinetics, the peak maximum time position t_m of an LM-OSL peak decreases slightly as a function of α. Therefore, the uniqueness of the t_m values continues to hold for any given value of T. Additionally, in the case of the LM-OSL curves, the constant values of the quantities ω/t_m, δ/t_m and τ/t_m could have a significant effect on the accuracy of the deconvolution analysis. The reason is rather simple. In all experimental LM-OSL curves there are points indicating the location of peaks. By considering these points as approximate values of t_m, and by using the values of $\omega, \delta, \tau/t_m$ from Eqs. (35), (36) and (38) (or directly from Table 2), one can evaluate the whole peak corresponding to the LM-OSL curve. This is very useful in practice, since it helps to drive the deconvolution analysis towards the correct solution.

Another significant difference between TL and LM-OSL CCDA analysis, is that in the case of TL it is not valid to accept that the best fit of a complex TL glow-curve corresponds to the lowest possible number of glow-peaks, since, as it was discussed above, at every TL peak maximum temperature T_m there corresponds an infinite number of TL peaks with differen E and s values. However, in the case of LM-OSL, the best fit with the lowest possible number of peaks could lead to a real solution, since at each t_m, it corresponds to one and only one LM-OSL peak. Therefore, the resolution is the main problem in the CCDA of LM-OSL.

The LM-OSL (and TL) analytical expressions can be used to analyze complex experimental LM-OSL (and TL) curves, provided that the superposition principle applies, i.e. that the net complex spectra is a linear superposition of independent processes.

The general-order TL/LM-OSL equations, although entirely empirical, are in fact interactive, since they include electron re-trapping, which of course involves all available electrons, and not only electrons that escaped from the main trap.

In the case of mixed-order kinetics, which is derived from the NMTS model, the interactive processes can be deduced from Eq. (12), which is common to both TL and LM-OSL. According to Eq. (12), the mixed-order expression tends to first-order kinetics when $n_{20} \gg n_{10}$, i.e. when a higher degree of competition is prevalent. Taking into account that for the derivation of mixed-order expression, it was assumed that $A_n = A_m$, it is concluded that the first-order kinetics limit of the mixed-order model is highly interactive. On the other hand, the mixed-order tends to second-order when $n_{20} \ll n_{10}$, i.e. when competition is not dominant. However, the assumption of $A_n = A_m$ remains, so that the second-order limit of the mixed-order expression is also interactive in its nature.

In the case of the IMTS model, all numerically derived simple TL/LM-OSL peaks are the result of strong trap interaction. The only case in which a single peak is an independent process is that resulting from zero re-trapping ($A_n = 0$) and no other traps are present ($N_2 = 0$), i.e, the first-order limit of OTOR model.

Table 2. Triangle assumption pseudo-constants and peak shape parameters of mixed-order LM-OSL peaks.

α	C_ω	C_δ	C_τ	ω/t_m	δ/t_m	τ/y_m
0.01	0.9715	0.9215	1.0484	1.6072	0.9262	0.6810
0.05	0.9703	0.9201	1.0490	1.6310	0.9479	0.6831
0.1	0.9680	0.9178	1.0491	1.6612	0.9760	0.6852
0.2	0.9636	0.9118	1.0500	1.7256	1.0363	0.6893
0.3	0.9555	0.9306	1.0508	1.7928	1.0999	0.6930
0.4	0.9456	0.8917	1.0511	1.8607	1.1650	0.6957
0.5	0.9319	0.8753	1.0510	1.9262	1.2286	0.6976
0.6	0.9139	0.8530	1.0512	1.9861	1.2868	0.6993
0.7	0.8904	0.8241	1.0511	2.0366	1.3368	0.7002
0.8	0.8611	0.7880	1.0515	2.0740	1.3729	0.7010
0.9	0.8269	0.7464	1.0518	2.0956	1.3490	0.7015
0.94	0.8118	0.7284	1.0512	2.0998	1.3986	0.7012
0.98	0.7967	0.7103	1.0515	2.1019	1.4003	0.7015

The net conclusion, therefore, is that the superposition principle applies strictly only to the first-order limits of the OTOR model, and also for general order kinetics. A CCD analysis will be valid strictly in well-isolated TL/LM-OSL peaks, and could also be valid in cases of slightly overlapping peaks. On the other hand, the validity of CCD analysis is questionable in cases of strong overlapping peaks.

To the best of our knowledge, this topic has received little attention in the TL/OSL literature, and there have not been any attempts to overcome this problem.

A general observation concerning the single peaks derived by a numerical solution of the differential equations, is that the geometrical shape of all peaks resulting from the OTOR, NMTS and IMTS models and representing any degree of trap interactions are contained in a restricted region of symmetry factor values between 0.42 and 0.52. This means that a unique value of the symmetry factor corresponds to many different trap interaction processes. Taking into account the degeneration of many interactive processes into a unique value of the symmetry factor, we believe that some of the uncertainties associated with the applicability of the superposition principle can be overcome by transforming the original $I\ (n_{10}, \alpha, \lambda, t)$ expressions into $I\ (I_m, t_m, \alpha, t)$ expressions. The reason is that the latter depends on I_m, t_m, which represent geometrical points of the experimental peaks, and on the single-valued parameter α, which is related to the symmetry of the peak.

4. Evaluation of Peak Shape Parameters by Numerical Simulation

The numerical simulations were performed using the mixed-order kinetic expression given by Eq. (15), taking into account Eqs. (16)–(18). In all simulations, it is taken $n_{10} = N_1$, since the geometrical shape parameters are independent of the ratio n_{10}/N_1. The values of the parameters used are $n_{10} = 10^5$ cm^{-3}, λ in the region 0.01–2 s^{-1}, and α in the region 0.05–0.99.

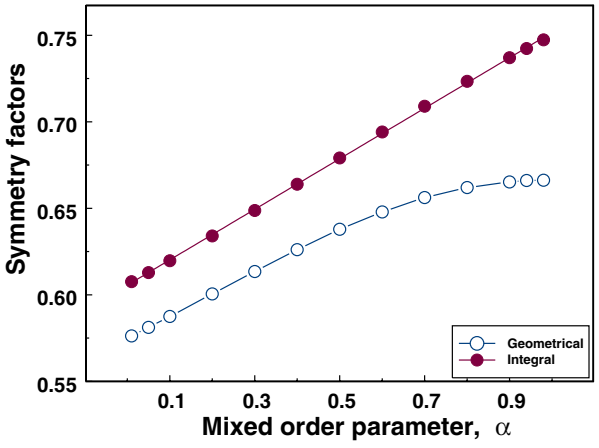

Fig. 2. The relation between the mixed-order parameter α and of the geometrical symmetry factors μ_g and integral symmetry factor $\mu'_g\alpha = -4.0883 + 6.7583\ \mu'_g$.

For each generated LM-OSL peak, all the geometrical shape parameters were evaluated and the results are as follows.

Figure 2 shows the geometrical and integral symmetry factors as a function of the mixed-order parameter α, with the corresponding numerical values listed in Table 1. The two symmetry factors show a different behavior as a function of α, which is quite similar to that found in the case of general-order kinetics.[6] On the contrary, in the case of TL, these differences were found to be small.[7] As seen in Fig. 2, there is an excellent linear relationship between the integral symmetry factor μ'_g and the mixed-order kinetics parameter α. The equation found is

$$\alpha = 6.7583\ \mu'_g - 4.0883 \qquad \text{or} \qquad \mu'_g = 0.1479\alpha + 0.605\,. \tag{47}$$

Figure 3 shows the triangle assumption pseudo-constants as a function of the mixed-order parameter α, whereas their corresponding numerical values are listed in Table 2. In the case of the pseudoconstant C_τ the behavior is similar to that previously found for general-order kinetics. However, the behavior of C_ω and C_δ is different from that of general order kinetics.[8]

Figure 4 shows the behaviors of ω/t_m, δ/t_m and τ/t_m respectively, whereas their numerical values are listed in Table 2. The behavior is exactly similar to that of general-order kinetics for α values up to 0.9.[8]

5. Comparison of Mixed-Order versus General-Order Expressions for Curve Fitting

General-order kinetics is widely used for analyzing TL and OSL data, but is not always accepted as a valid model, due to its pure empirical nature. On the other hand, the mixed-order kinetics model has a physical basis, but is almost never

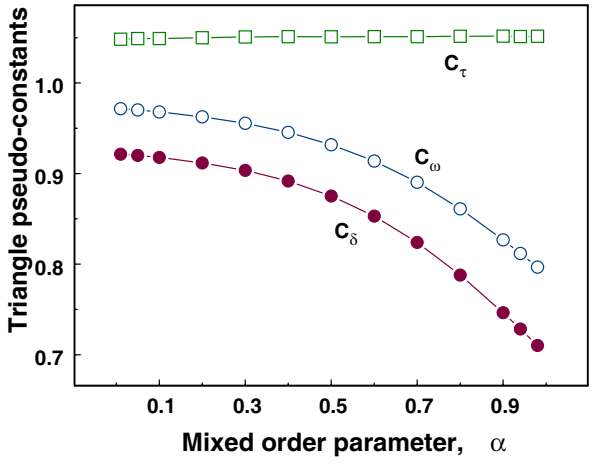

Fig. 3. The triangle assumption pseudo-constants C_ω, C_δ and C_τ as a function of the mixed-order parameter α.

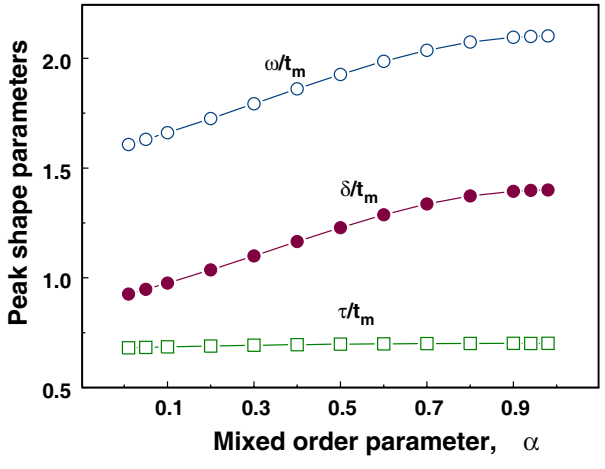

Fig. 4. The peak shape parameters ω/t_m, δ/t_m, and τ/t_m, as a function of mixed-order parameter α.

used for data analysis. In order for CCD analysis to become a routine tool for analyzing experimental results, it is important for the TL/OSL community to adopt a generally accepted single peak model.

It is desirable that the differences between the empirical general-order and the physically meaningful mixed-order be as small as possible.

There are some other interesting quantities which are evaluated during the numerical simulations in this paper, which are very useful for the curve fitting procedure and for a comparison between mixed- and general-order kinetics. These are the term F_m given by Eq. (14) for $t = t_m$, the term $(F_m + \alpha)/F_m$, called hereafter b_{mix},

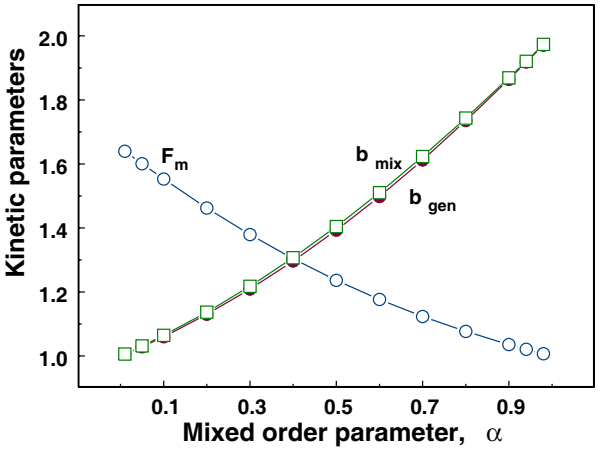

Fig. 5. Kinetic parameters as a function of the mixed-order parameter α. $F_m = 1.6476 - 1.0012\alpha + 0.357\alpha^2$, $b_{\rm mix}=(F_m + \alpha)/F_m$, and $b_{\rm gen}$ the general kinetic order of a mixed-order LM-OSL peak having the same integral symmetry factor μ'_g.

which is a common term in Eqs. (35), (36) and (38) and finally the general-order parameter b, which is related to the integral symmetry factor of a LM-OSL peak. For the case of general-order kinetics, the integral symmetry factor (see Eq. (33)) is given by the equation[7]

$$\frac{n_{1m}}{n_{10}} = \mu'_g = \left(\frac{2b}{b+1}\right)^{\frac{1}{1-b}} . \tag{48}$$

Once the integral symmetry factor μ'_g is evaluated during the simulations, the corresponding general-order parameter b is evaluated through Eq. (48) by an iteration method.[7]

The results are shown in Fig. 5 and the numerical values are listed in Table 1. As it is seen in Fig. 5, the mixed-order kinetics factor $b_{\rm mix}$ for LM-OSL almost coincides with the general-order kinetic parameter b. The relation between F_m and α is very important for the practical use of the deconvolution functions given in this paper. The mathematical expression found from the simulated data in Fig. 5 is

$$F_m = 1.6476 - 1.0012\alpha + 0.357\alpha^2 . \tag{49}$$

Obviously, a similar relation exists also between the term F_m and the integral symmetry factor μ'_g, since the latter is linearly related to α though Eq. (47).

All curve fittings were performed using the MINUIT computer program,[9] while the goodness of fit was tested using the Figure Of Merit (FOM)[10] given by:

$$\text{FOM} = \sum \frac{Y_{\rm Exper} - Y_{\rm Fit}}{A} , \tag{50}$$

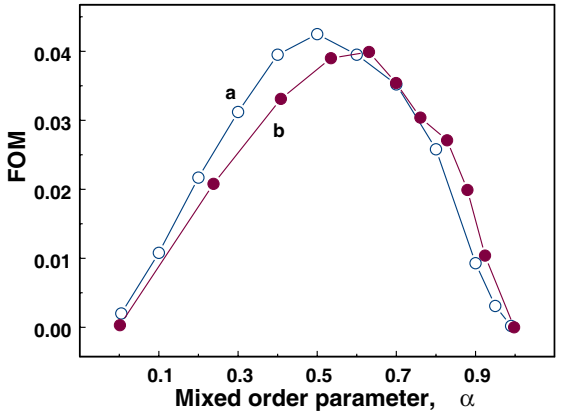

Fig. 6. FOM values resulting from (a) the fitting of a general order LM-OSL peak using a mixed-order kinetics expression and from (b) the fitting of mixed-order kinetics LM-OSL peak using a general order kinetics expression.

where Y_{Exper} is the experimental glow-curve, Y_{Fit} is the fitted glow-curve and A is the area of the fitted glow-curve.

The deconvolution function given by Eq. (42) is in fact a transformation of the main deconvolution function given in Eq. (15). The curve-fitting procedure on synthetic LM-OSL peaks generated by Eq. (15), by both alternatives of Eq. (42), gave FOM values of the order of 10^{-5} and better, which means that these equations coincide numerically with each other in the range of parameters studied.

The comparison between general- and mixed-order kinetics is performed as follows. Synthetic general-order LM-OSL curves were fitted using the mixed-order deconvolution function in Eq. (42), and synthetic mixed-order LM-OSL peaks were fitted by a general-order de-convolution function.[8] The results are shown in Fig. 6, where it is seen that the fitting accuracy of the two types of kinetics decreases in the intermediate region between first and second-order. The effectiveness of both kinds of deconvolution functions to fit each other is more or less the same, and in the worst case the FOM is less than 0.04 (4%). The curve fitting of mixed-order LM-OSL curves with a general-order function gives the respective kinetic order b, whereas the curve-fitting of general-order curves with a mixed-order function gives the respective mixed-order parameter α. The results are shown in Fig. 7, where one can see that the expressions for each kind of kinetics evaluates the kinetic parameter of the other type with very good accuracy.

A comparison of the fitting of a LM-OSL curve with mixed-order and general-order kinetics is shown in the upper part of Fig. 8 for the case of the worst FOM (4%). The differences are not easily visible in the figure. The difference obtained by subtracting the general-order from the mixed-order fitting curve is given in the lower part of Fig. 8. This difference is always less than 4%, in agreement with the FOM values of Fig. 7.

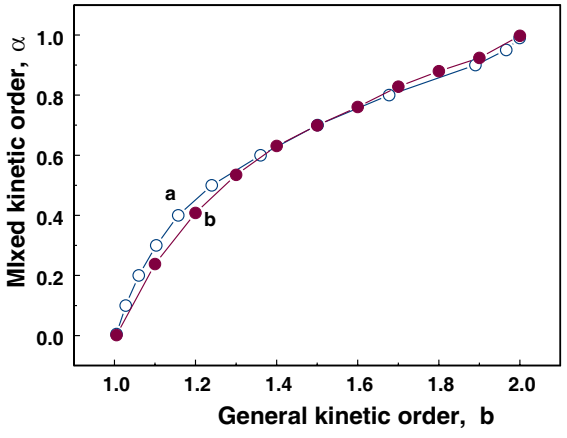

Fig. 7. Relation between mixed-order parameter α and general order kinetic b resulting from (a) the fitting of a general order LM-OSL peak using a mixed-order kinetics expression and from (b) the fitting of mixed-order kinetics LM-OSL peak using a general order kinetics expression.

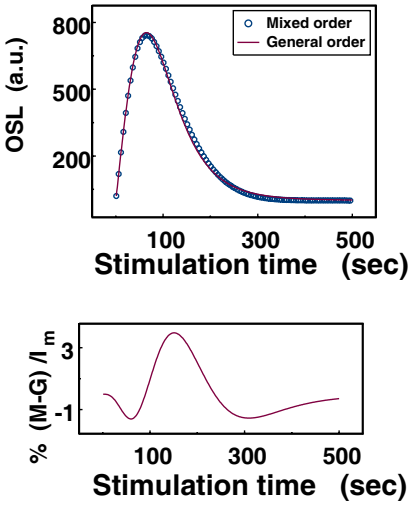

Fig. 8. A comparison example of a mixed-order kinetics LM-OSL peak with a general-order kinetics LM-OSL peak for $\alpha = 0.5$, which corresponds to the worst FOM value of Fig. 6. The difference between the mixed-order kinetics LM-OSL peak and the general-order kinetics LM-OSL peak normalized to peak maximum intensity.

6. Conclusions

Analytical expressions for mixed-order LM-OSL peaks were derived by applying the appropriate assumptions on the differential equation governing the OSL process. Similarly, an analytical expression describing a CW-OSL curve was also derived along with its transformation equation into a peak shaped PS-LM OSL curve.

Furthermore, the original LM-OSL expression of the form $I\ (n_{10}, \alpha, \lambda, t)$ was transformed into an expression of the form $I\ (I_m, t_m, \alpha, t)$, which depended upon variables that can be extracted directly from the experimental LM-OSL and PS-LM OSL data.

The geometrical characteristics (symmetry factors and triangle assumption pseudo-constants) of LM-OSL peaks were studied in detail. The relations between ω, δ, τ and the time maximum position t_m of the LM-OSL peaks were derived, and were evaluated as a function of the mixed-order parameters α.

Finally, a comparison between general- and mixed-order analytical expressions was performed by using a curve fitting procedure. By fitting general-order LM-OSL peaks with a mixed-order analytical expression and vice-versa, it was found that the analytical expression of each kind of kinetics evaluates the kinetic parameter of the other with very good accuracy.

References

1. E. Bulur, *Radiat. Meas.* **26** (1996) 701.
2. E. Bulur, *Radiat. Meas.* **32** (2000) 141.
3. R. Chen and S. W. S. McKeever, *Theory of Thermoluminescence and Related Phenomena* (World Scientific, 1997).
4. C. M. Sunta, W. E. F. Ayta, J. F. D. Chubaci and S. Watanabe, *Radiat. Meas.* **35** (2002) 47.
5. R. Chen, *J. Appl. Phys.* **40** (1969) 570.
6. G. Kitis and V. Pagonis, *Nucl. Instr. Meth. Phys. Resear. B* **262** (2007) 313.
7. G. Kitis, R. Chen and V. Pagonis, *Phys. Stat. Sol. A* **205** (2008) 1181.
8. G. Kitis and V. Pagonis, *Radiat. Meas.* **43** (2008) 737.
9. F. James and M. Roos, *MINUIT, CERN Program Library Entry D506*, 1977, http://root.cern.ch.
10. H. G. Balian and N. W. Eddy, *Nucl. Instrum. Methods* **145** (1977) 389.